



Micro injection of metallic glasses parts under ultrasonic vibration



X. Liang^{a,b}, J. Ma^{a,*}, X.Y. Wu^{a,*}, B. Xu^a, F. Gong^a, J.G. Lei^a, T.J. Peng^a, R. Cheng^a

^a Guangdong Provincial Key Laboratory of Micro/Nano Optomechatronics Engineering, College of Mechatronics and Control and Engineering, Shenzhen University, Shenzhen 518060, China

^b Shenzhen ESUN Exhibition Company Limited, Shenzhen 518048, China

ARTICLE INFO

Article history:

Received 1 September 2016

Received in revised form 9 October 2016

Accepted 11 October 2016

Available online 21 December 2016

Keywords:

Metallic glasses

Micro injection

Ultrasonic vibration

ABSTRACT

This work investigates the evolution of structure and mechanical performance of metallic glasses (MGs) under a proposed rapid forming approach. Through the unique ultrasonic-assisted micro injection method, micro MGs parts with fine dimensional accuracy were successfully fabricated. The temperature during the micro injection is higher than the glass transition temperature and lower than the crystallization temperature. Differential scanning calorimeter curve and X-ray diffraction pattern show that the MGs micro parts keep the amorphous nature after the ultrasonic-assisted micro injection. Our results propose a novel route for the fast forming of MGs and have promising applications in the rapid fabrication of micro scale products and devices.

© 2017 Published by Elsevier Ltd on behalf of The editorial office of Journal of Materials Science & Technology.

1. Introduction

In the early 1970s, the Japanese researchers placed the ultrasonic oscillator on the nozzle of the injection molding equipment to form excellent plastic parts with free residual stress [1]. Inspired by their idea, researchers developed an ultrasonic injection molding system and processing technology for the injection molding with short cycle times [2,3]. Afterwards, the ultrasonic plasticization forming technology already obtained wide applications in the fields of medical treatment, telecommunication, and optics *etc.*

In the study of ultrasonic plasticization molding, researchers have successfully made use of a low-power ultrasound with a frequency of 20 kHz to conduct macro-scale compression molding experiments on thermosetting (phenolics and allylics) and thermoplastic (acrylics and vinyls) powder [4]. Later, ultrasonic plasticization molding method was used to experimentally fabricate micro parts through raw materials of polylactide (PLA) [5], polybutylene succinate (PBS) [6], polypropylene (PP) [7], and ultra-high molecule weight polyethylene (UHMWPE) [8,9] powders.

In addition, metallic powders were also used as the raw materials of the ultrasonic-assisted micro injection method (UMIM). For instance, Wu et al. took low-melting-point Sn-Bi eutectic alloy powder as the raw material to fabricate three kinds of micro gears with different specifications by micro ultrasonic molding process

[10,11]. In similarity with the studies of Wu et al., Luo et al. [12] also utilized 42%Sn–58%Bi eutectic alloy powder, copper powder and copper fiber as the raw materials to fabricate semi-finished micro parts by micro ultrasonic molding process and the parts were lately heated to a certain temperature for some hours. The ultimately fabricated micro parts have been proved better in terms of thermal performance and mechanical properties, compared with the semi-finished ones.

However, as an emerging material by combining both advantages of plastics and metals, the UMIM for metallic glasses (MGs) have not been studied since its discovery in 1960s [13]. The unique properties of MGs, such as high strength, high specific strength, large elastic strain limit, and excellent wear and corrosion resistances along with other remarkable engineering properties, have attracted significant interest for both sciences and industrial fields [13,14]. One of the most intriguing features of MGs is their ability to be thermoplastically formed like plastics above the glass transition temperature T_g . This “thermoplastic forming” ability was widely perceived as finally bridging the gap between the manufacturing of metals and that of plastics [15–21]. Because of this ability, bulk metallic glasses (BMGs) can be formed into parts of complex surface structures with a well-defined geometry and shape on length scales ranging from macro, micro, to even nano [22–24]. Accordingly, researchers have exploited different conventional thermoplastic techniques, such as hot embossing [25,26], blow molding [27] and injection molding [28], to fabricate various structures and products using BMGs. For example, Li et al. [29,30] have made great efforts on this direction. It is widely accepted that thermoplastic forming is

* Corresponding authors.

E-mail addresses: majiang@szu.edu.cn (J. Ma), wuxy@szu.edu.cn (X.Y. Wu).

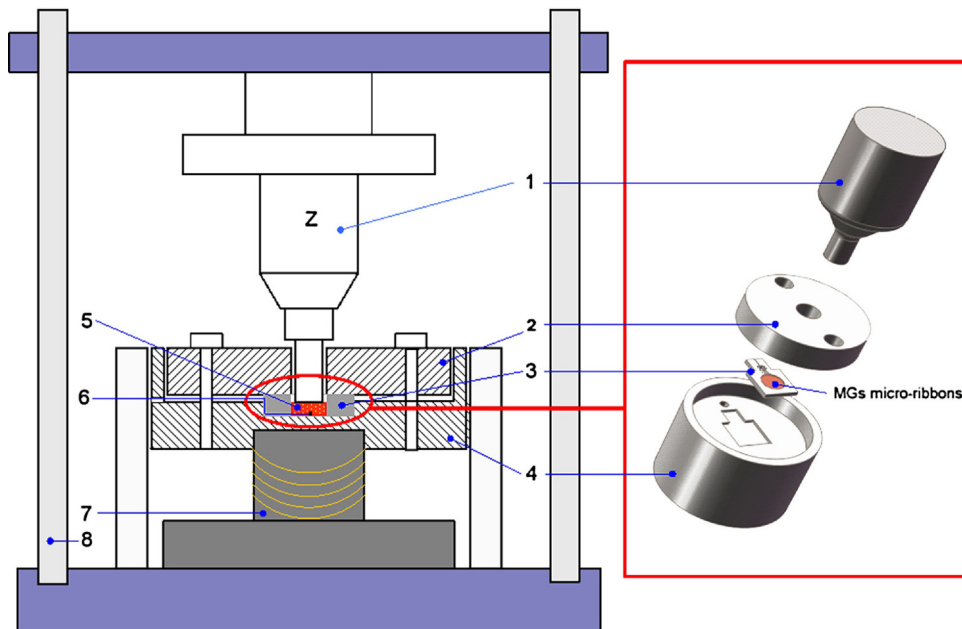


Fig. 1. Schematic diagram of UMIM setup (1—Ultrasonic sonotrode; 2—Cover plate with charging barrel; 3—Mold insert with microstructure; 4—Baseplate; 5—MGs micro-ribbons; 6—K-type thermocouple; 7—Resistance heating furnace; 8—Mechanical testing system).

one of the most promising fields for the application of BMGs. Compared with the thermoplastic micro embossing, the micro injection forming could have very high efficiency and low cost. Therefore, to develop the injection forming technique is significant for the applications of MGs.

In the present work, the UMIM is introduced for the micro injection of MGs. The fabricated MGs micro parts have fine dimensional accuracy and excellent mechanical performance. Furthermore, after UMIM the MGs parts remain their amorphous nature, which have been verified by the X-ray diffraction (XRD) pattern and differential scanning calorimeter (DSC) curves. Our results evidence a novel route for the fast forming of MGs and have promising applications in the rapid fabrication of micro scale products and devices.

2. Experimental details

2.1. Raw materials

The raw material is La-based MGs ribbon with a thickness of 40 μm (the composition of the material is $\text{La}_{55}\text{Ni}_{20}\text{Al}_{25}$, La 55 at.%, Ni 20 at.%, and Al 25 at.%), which was prepared by the melt-spun method. The MGs ribbon was cut into grains with a length of less than 1 mm by mechanical shearing.

2.2. UMIM approach

Fig. 1 is the schematic diagram of UMIM. Firstly, the resistance heating furnace was started and the mold insert with microstructure was heated to a proper temperature T of 200 $^{\circ}\text{C}$ to enhance the flow ability during the micro injection. Secondly, the MGs micro-ribbons were pre-filled into the charging barrel hole in the middle of cover plate and, after then, the micro-ribbons were repeatedly compacted by ultrasonic sonotrode with a load of 0.5 kN. Thirdly, a mechanical testing system (Zwick, Roell, Z0.5) was performed and the process was preloaded to 4.0 kN at a speed of 1 mm min^{-1} to form an MGs billet. Fourthly, after setting ultrasonic duration time t_u , the ultrasonic vibration started and the MGs micro-ribbons were compacted at a speed of 1 mm min^{-1} to a load of 5.0 kN by the mechanical tester. The soft MGs micro-ribbons were filled into

the micro cavity under the load of the ultrasonic sonotrode and eventually a UMIM part was formed.

2.3. Methodology

The amorphous nature of the La-based MGs ribbon and UMIM parts were ascertained by XRD (Bruker D8 Advanced) with $\text{CuK}\alpha$ radiation and DSC (Perkin–Elmer DSC 8000) at a heating rate of 20 K min^{-1} . The surface morphology was explored on a scanning electron microscope (SEM, Hitachi SU70).

The flat surfaces of the UMIM parts were tested using a nanoindenter (Agilent key-sight G200) with a standard Berkovich nanoindentation tip. To limit the influence of viscoelastic creep, the nanoindentation test procedures involved several loading, unloading, and holding segments until a fixed depth of 2000 nm were achieved. The process ended with complete unloading. The loading and unloading segments were performed at a speed of 10 nm s^{-1} .

A high speed (1000 points per second) temperature measurement module, which was composed of K-type thermocouples (Omega TC-TT-K-36-36) and a data acquisition card (NI USB 9213), was built to record the temperature curves at the bottom of micro parts during the UMIM process. The layout of the K-type thermocouple is shown in **Fig. 1**.

3. Results and discussion

3.1. Measurement of replication rate by SEM

The overall appearance of La-based UMIM parts and micro mold cavity were observed by SEM. **Fig. 2**(a and b) shows the microstructure of the micro cavities that were used as mold during the UMIM process. The cross-section of the UMIM part is presented in **Fig. 2**(c). No forming defects such as porosities or bonding boundaries can be found, indicating a good bonding quality of the MG ribbons. From the details in **Fig. 2**(d–f), it can be seen that the MGs were nearly fully filled into the mold cavity, including the micro corner. The excellent forming condition indicates the superior filling ability of MGs under the micro injection molding. To quantitatively evaluate the replication condition, we adopted the replication rate α ,

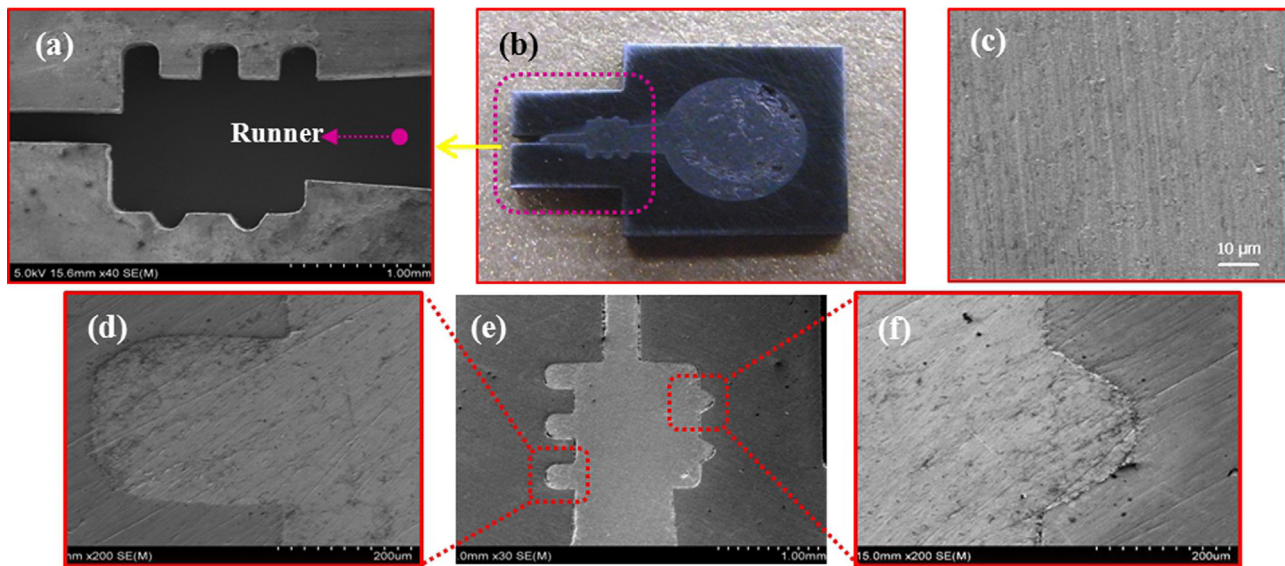


Fig. 2. SEM images of the samples: (a) and (b) are the micro cavities with microstructure; (c) is the cross-section of UMIM part; (d), (e) and (f) are UMIM parts.

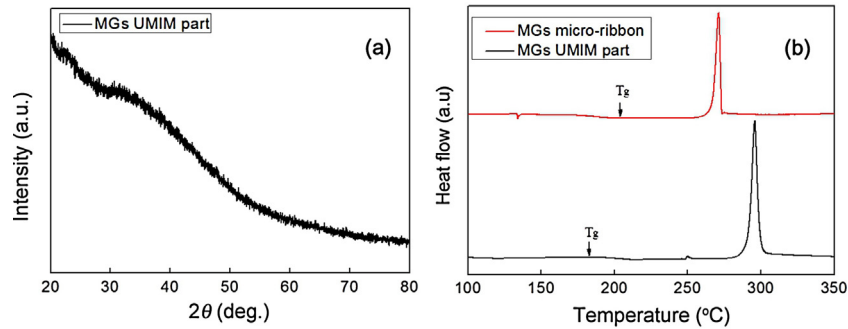


Fig. 3. XRD (a) and DSC (b) curves of the UMIM part.

expressed as: $\alpha = A_2/A_1 \times 100\%$ (where A_1 and A_2 are the areas of the micro cavity and UMIM MGs parts, respectively). Based on this equation, $\alpha = 98.40\%$, that is to say that the MGs replica is in good accordance with the micro mold.

3.2. Densities

The weight (W_1) of MGs ribbons and UMIM parts were measured in the air with an electronic balance (Sartorius Quintix35-1CN, measurement accuracy 0.01 mg) and, after then, their weight (W_2) in the analytical pure alcohol was measured. According to the formula:

$$\rho = W_1 \cdot \rho_1 / (W_1 - W_2) \quad (1)$$

where the density ρ_1 is 0.802 g ml^{-1} . The density measurement was repeated for five times and the calculated average densities of the MGs ribbons and the UMIM parts were 6.087 and 5.861 g mm^{-3} , respectively, similar to the bulk one as mentioned in reference [31]. The measurement error was controlled in $\pm 0.2\%$. The results imply that the MGs ribbons are completely bonded together as a whole during the UMIM.

3.3. DSC and XRD analysis

It is important to check whether or not the UMIM parts remain amorphous after the micro injection forming. In Fig. 3(a), XRD pattern of La-based UMIM part was measured by a wide-angle XRD at a scanning speed of 5 deg./min . As shown in Fig. 3(b), the

DSC curves of La-based MGs UMIM part and MGs micro-ribbon treated by increasing the temperature with a rate of 10 K min^{-1} accordingly indicate that the glass transition temperatures T_g were 186.45 and 200.35°C while the crystallization temperatures T_x were 271.12 and 295.83°C , respectively. The deviation range of T_g and T_x between the ribbon and UMIM part is about only 5.00°C . No crystallization was found for the UMIM part. The invariance of structure is the basic requirement of thermoplastic forming for MGs, thereby ensuring the mechanical performance of the as-fabricated micro parts.

3.4. Micromechanical properties of the UMIM parts using nanoindentation tests

To examine the mechanical performance of the La-based MGs parts after UMIM, the nanoindentation tests were conducted on their surfaces using an Agilent key-sight G200 in situ nanomechanical testing instrument with a standard Berkovich nanoindentation tip. The local elastic modulus E_r and local hardness H on the La-based MGs and the surface of the UMIM part were recorded, as compared in Fig. 4(a) and (b). The E_r of the La-based MGs in the nanoindentation tests ranges from 43.3 to 48.1 GPa , with a standard deviation of 1.70 GPa , and the hardness value of H is a range between 2.43 and 2.93 GPa , with a standard deviation of 0.17 GPa in Fig. 4(a). The E_r of the UMIM part in the nanoindentation tests ranges from 53.92 to 64.80 GPa with a standard deviation of 3.05 GPa , and the H value of is between 2.71 and 3.65 GPa with a standard deviation of 0.28 GPa in Fig. 4(b). It should be noticed that

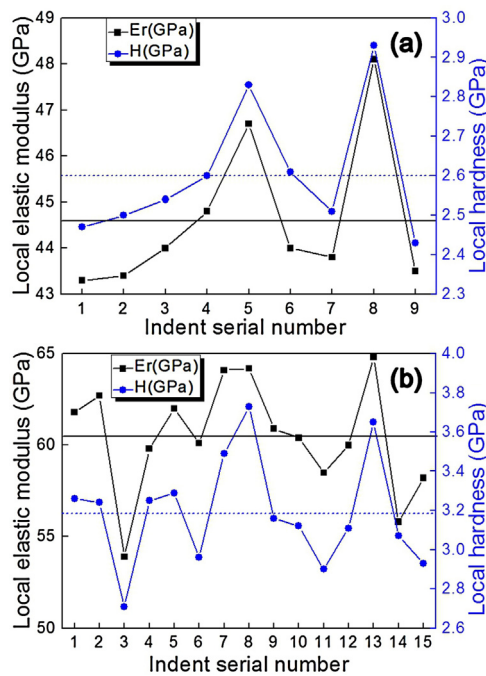


Fig. 4. Distribution of modulus E_r and hardness H of the La-based ribbons (a) and the UMIM part (b). The black solid line is the mean value of E_r , and the blue short dash line is the mean value of H .

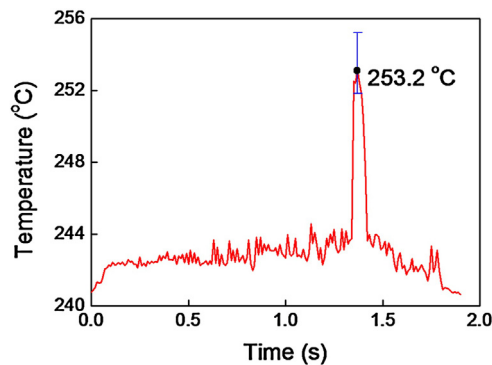


Fig. 5. Temperature curve of MGs micro-ribbons during UMIM.

the elastic modulus E_r and the local hardness H of the UMIM part is higher than those of the original ribbons, which might be attributed to the fact that the ultrasonic vibration induced a hard layer on the surface of metallic glass, similar to the shot peening effect. From the result of the micromechanics test mentioned above, the mechanical performance of MGs did not decay after the UMIM, being even better than that of the original ribbons [31].

3.5. Temperature measurement

A very thin gauge thermocouple wire coupling with a high rate of data acquisition was used to detect the temperature change during the UMIM process, and the temperature curve is presented in Fig. 5. It can be seen that the temperature of MGs ribbons increased up to 253.2°C (the deviation ranges from +2.1 to −1.3°C) rapidly in a very short time when the ultrasonic vibration started, the MGs ribbons became soft at this temperature and filled into the micro mold, forming the injection parts.

According to the heat equation, $Q = m \times C \times \Delta t$ where m , C and Δt are the mass, specific heat capacity and temperature raise of an object when given a heat Q , respectively. In this case, the values of

m , C and Δt are 0.095 g, $0.263 \text{ J} (\text{gK})^{-1}$ and 228°C (room temperature 25°C), respectively. Therefore, the heat quantity needed to drive the MGs sample to 253.2°C would be about 5.69 J. On the other hand, the work done by the ultrasonic indenter could be calculated by the following equation:

$$W = F \times (f \times t \times i) \quad (2)$$

where F is the applying force of the ultrasonic indenter ($F = 5000 \text{ N}$), and $f = 20000$, $t = 2.0 \text{ s}$ and $i = 5.0 \mu\text{m}$, which are the beating frequency, forming time and displacement per beating of the ultrasonic indenter, respectively. By substituting the above values in Eq. (2), we obtain $W = 1000 \text{ J}$, which is much greater than the required heat quantity Q , indicating that the ultrasonic beating could provide enough energy for the MGs to get soft. The energy provided by the ultrasonic indenter can be divided into two parts: one is used to heat up the MGs sample into its super cooled liquid region and the other one is dissipated by the deformation after it gets soft.

4. Conclusion

In this work, a novel UMIM method for the La-based MG ribbons was proposed and the MG part with fine micro structures was successfully fabricated by this approach. XRD and DSC measurements suggest that no crystallization occurred during the UMIM process, which is in accordance with the temperature detection. The maximum temperature reaches 253.2°C by a real-time temperature monitor, lower than the crystallization temperature. Furthermore, the replication rate of the UMIM parts is as high as 98.4% compared with the mold cavity. The densities of the ribbons and the UMIM parts were measured to be 6.087 and 5.861 g mm^{-3} , respectively, reflecting the good bonding quality. The elastic modulus and hardness of the MG ribbon and UMIM part were also tested by the nanoindentation, respectively. Our results put forward a fast injection method for MG parts and may throw light on the extensive application of MGs.

Acknowledgments

This work is supported by the National Natural Science Foundation of China (Nos. 51605304, 51575360, 51375315 and 51405306), the China Postdoctoral Science Foundation (No. 2016M601423), the Ph.D. Start-up Fund of Natural Science Foundation of Guangdong Province (Nos. 2016A030310036 and 2016A030310043), the Major Science and Technology Project of Guangdong Province (No. 2014B010131006), and the Science and Technology Innovation Commission of Shenzhen (Nos. JCYJ20150525092941026, JCYJ20150625102923775, JCYJ20140418095735629 and JSGG20140519104809878). The authors are grateful to C. Z. Wu and J. X. Lu for their essential contribution to the work.

References

- [1] Itaya Seisakusho KK, Injection moulding apparatus with an ultrasonic oscillator on the injection nozzle, Japanese Patent, JP70006949-B, 1970.
- [2] W. Michaeli, A. Spennemann, R. Gärtner, *Microsyst. Technol.* 8 (2002) 55–57.
- [3] W. Michaeli, T. Kamps, C. Hopmann, *Microsyst. Technol.* 17 (2011) 243–249.
- [4] H.V. Fairbanks, *Ultrasonics* 12 (1974) 22–24.
- [5] M. Sacristá, X. Plantá, M. Morell, J. Puiggali, *Ultrason. Sonochem.* 21 (2014) 376–386.
- [6] M. Planellas, M. Sacristán, L. Rey, C. Olmo, J. Aymami, M.T. Casas, L.J. Del Valle, L. Franco, J. Puiggali, *Ultrason. Sonochem.* 21 (2014) 1557–1569.
- [7] K. Zeng, X.Y. Wu, X. Liang, B. Xu, Y.T. Wang, X.Q. Chen, R. Cheng, F. Luo, *Int. J. Adv. Manuf. Technol.* 70 (2014) 515–522.
- [8] X. Liang, X.Y. Wu, K. Zeng, B. Xu, S.Y. Wu, H. Zhao, B. Li, S.C. Ruan, *J. Micromech. Microeng.* 24 (2014) 045014.
- [9] X. Liang, X.Y. Wu, B. Xu, J. Ma, Z.Y. Liu, T.J. Peng, L.Y. Fu, *J. Micromech. Microeng.* 26 (2016) 015014.

- [10] S.Y. Wu, X.Y. Wu, B. Xu, R. Cheng, F. Luo, S.C. Ruan, *J. Mater. Process. Technol.* 214 (2014) 2668–2675.
- [11] S.Y. Wu, X.Y. Wu, B. Xu, X.Q. Chen, R. Cheng, S.C. Ruan, *Int. J. Adv. Manuf. Technol.* 79 (2015) 897–904.
- [12] W.Y. Luo, X.Y. Wu, S.Y. Wu, B. Xu, R. Cheng, S.C. Ruan, *J. Mater. Process. Technol.* 223 (2015) 313–318.
- [13] W. Klement, R.H. Willens, P. Duwez, *Nature* 187 (1960) 869–870.
- [14] A.L. Greer, *Science* 267 (1995) 1947–1953.
- [15] J. Schroers, *Adv. Mater.* 22 (2010) 1566.
- [16] X.Q. Gao, W.H. Wang, H.Y. Bai, *J. Mater. Sci. Technol.* 30 (2014) 546–550.
- [17] Y. Saotome, K. Imai, S. Shioda, S. Shimizu, T. Zhang, A. Inoue, *Intermetallics* 10 (2002) 1241–1247.
- [18] N. Li, T. Xia, L.P. Heng, L. Liu, *Appl. Phys. Lett.* 102 (2013) 251603.
- [19] J.P. Chu, H. Wijaya, C.W. Wu, T.R. Tsai, C.S. Wei, T.G. Nieh, *J. Wadsworth, Appl. Phys. Lett.* 90 (2007) 034101.
- [20] G.C. Ma, Z.W. Zhu, Z. Wang, H.F. Zhang, *J. Mater. Sci. Technol.* 31 (2015) 941–945.s
- [21] W. Zhou, W.P. Weng, J.X. Hou, *J. Mater. Sci. Technol.* 32 (2016) 349–354.
- [22] A. Inoue, A. Takeuchi, *Acta Mater.* 59 (2011) 2243–2267.
- [23] W.H. Wang, *Adv. Mater.* 21 (2009) 4524–4544.
- [24] G. Kumar, H.X. Tang, J. Schroers, *Nature* 457 (2009) 868–872.
- [25] J. Ma, X. Zhang, W.H. Wang, *J. Appl. Phys.* 112 (2012) 024506.
- [26] J. Ma, X.Y. Zhang, D.P. Wang, D.Q. Zhao, D.W. Ding, K. Liu, W.H. Wang, *Appl. Phys. Lett.* 104 (2014) 173701.
- [27] J. Schroers, T.M. Hodges, G. Kumar, H. Raman, A.J. Barnes, Q. Pham, T.A. Waniuk, *Mater. Today* 14 (2011) 14–19.
- [28] A. Wiest, J. Harmon, M. Demetriou, R. Daleconner, W.L. Johnson, *Scr. Mater.* 60 (2009) 160–163.
- [29] N. Li, X.N. Xu, Z.Z. Zheng, L. Liu, *Acta Mater.* 65 (2014) 400–411.
- [30] N. Li, W. Chen, L. Liu, *JOM* 68 (2016) 1246–1261.
- [31] W.H. Wang, *Prog. Mater. Sci.* 57 (2012) 487–656.